Effect of passive plates on vertical instability in the EAST tokamak*

Liu Guang-Jun(刘广君)†, Wan Bao-Nian(万宝年), Qian Jin-Ping(钱金平),
Sun You-Wen(孙有文), Xiao Bing-Jia(肖炳甲), Shen Biao(沈 飚),
Luo Zheng-Ping(罗正平), Ji Xiang(戟 翔), and Chen Shu-Liang(陈树亮)

Institute of Plasma Physics, Chinese Academy of Sciences, Hefei 230031, *China*

(Received 15 December 2011; revised manuscript received 4 January 2012)

The effect of passive plates on vertical displacement control in the EAST tokamak is investigated by open loop experiments and numerical simulations based on a rigid displacement model. The experiments and simulations indicate that the vertical instability growth rate is reduced by a factor of about 2 in the presence of the passive plates, where the adjacent segments are not connected to each other. The simulations also show that the vertical instability growth rate is reduced by a factor of about 10 if all adjacent segments on each passive plate loop are connected to each other. The operational window is greatly enlarged with the passive plates.

Keywords: passive plate, vertical instability, rigid displacement model

PACS: 52.75.–d, 52.35.Py, 52.65.–y **DOI:** 10.1088/1674-1056/21/8/085201

1. Introduction

Future tokamaks such as ITER will have an elongated cross section, because plasma elongation can improve the ratio of tokamak performance-to-cost. However, these plasmas are inherently unstable against vertical displacement. The loss of vertical position control will lead to plasma moving into the vacuum chamber, resulting in disruption and damage to the in-vessel components. Good control of vertical instability is necessary for reliable plasma operation.[1,2] Vertical instability control normally contains two strongly coupled parts: the active control and the passive control systems.[3] The active control is realized by external poloidal field (PF) coils, while passive control stems from the stabilizing effect of the conducting structures of the vacuum vessel or built-in vessel components. A passive control system can impede fast vertical displacements, while PF coils are used to control slow displacement drift. Some of the discharges in tokamaks are out of control because of vertical instability, which is caused by the long response time of the active control system and partially due to relatively weak coupling between plasma and active/passive structures.

The Experimental Advanced Superconducting Tokamak (EAST) is a full superconducting tokamak with D-shaped cross-section plasma, which is similar to ITER's configuration. There are several reasons for the control of vertical instability to be more difficult on EAST than on a conventional tokamak. Strong coupling between superconducting PF coils and the shielding effects of the in-vessel wall make the response time of the active control system relatively long; the long distance between the PF coils and plasma, due to the thick thermal shielding, relatively weakens their coupling.[4,5]

In 2010, a passive plate system was designed and built in EAST to improve the control of vertical instability. Compared with an active feedback control system, a passive plate is less expensive and complex, but more sensitive to fast vertical displacement. It can reduce the growth rate of vertical instability and lower the requirements for the response time of the active feedback control system. Stabilization effects of the vacuum vessel on vertical instability have been discussed in Refs. [5] and [6]. In this paper, the stabilization effect of passive plates on vertical instability is studied by comparing the experimental observation with the numerical simulation based on a rigid displacement model,[3,7,8] which has been validated and used in the investigation of vacuum vessel effects on vertical instability.[9] We extend it by including the

*Project supported by the National Natural Science Foundation of China (Grant Nos. 10725523, 10721505, and 10835009).
†Corresponding author. E-mail: gjliu@ipp.ac.cn
© 2012 Chinese Physical Society and IOP Publishing Ltd

passive plate.

The rest of the present paper is organized as follows. The passive structure in EAST is introduced in Section 2, and the open loop experiments with passive plates are presented in Section 3. Some predictions of the effect of passive plates on vertical instability based on numerical simulations are discussed in Section 4. Finally, the conclusion is drawn in Section 5.

2. Passive structure on EAST

EAST is designed to be up–down symmetric, as shown in Fig. 1. It is equipped with a set of 14 superconducting PF coils around the vacuum vessel and a pair of water-cooled copper coils inside the vacuum vessel (IC). The positions of the two passive plate loops are also shown in the figure.

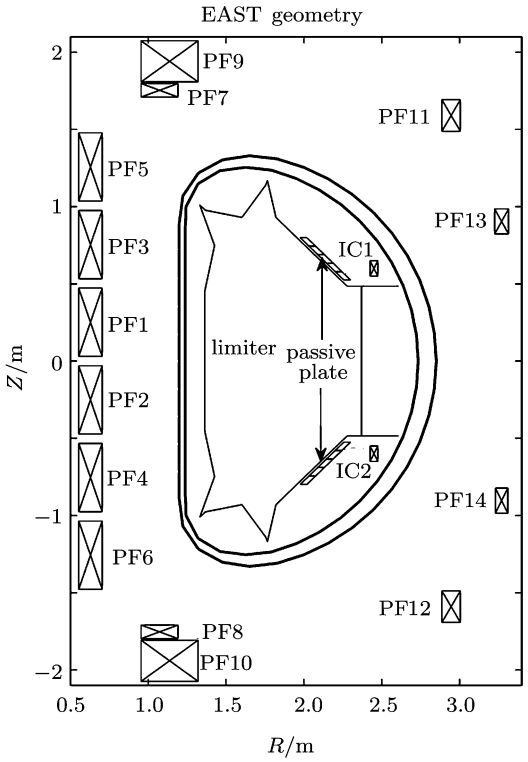


Fig. 1. Arrangement of the 14 PF coils (PF 1–14), active feedback coils (IC1, IC2), and the passive plate loops on the poloidal cross section of EAST.

Figure 2 shows the designed passive plate loops on EAST.[10] They are made of copper alloy. Each loop has 8 segments with 30 mm in thickness and 350 mm in width. The adjacent segments of each loop are connected to each other by 8-mm thick copper alloy plates except a gap for current bridge. A coaxial cable will be used as a current bridge to connect the two loops to form a saddle circle. The designed resistance of each passive plate loop is 75.6 μΩ. The passive plate in this case is defined as case A.

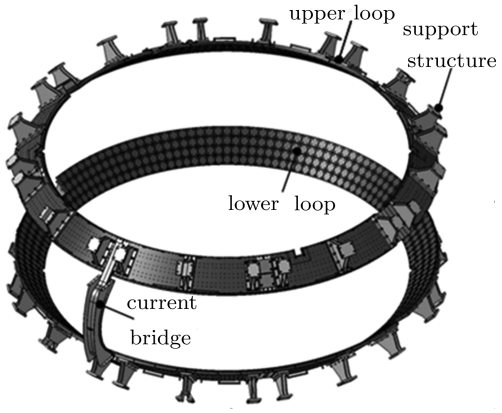


Fig. 2. Designed structure of the passive plate on EAST.

Presently, the current bridge is not connected and the adjacent segments of each loop are not connected to each other directly. However, all the segments are connected to vacuum vessel via the supporting structures to form loops. The estimated resistance of each loop is 1 mΩ ∼ 3 mΩ. The passive plate in this case is defined as case B. The case without passive plates is case C for comparison.

3. Open loop experiments in comparison with simulations

3.1. Experimental set-up

The open loop experiments are carried out in case B to detect the growth rate of vertical instability. As shown in Fig. 3, the proportional–integral–differential (PID) feedback gains for vertical position are set to be zero at 4 s; thereafter the IC current is switched off (Fig. 3(b)) and plasma control system releases the control for vertical position. The plasma vertical position drifts exponentially from its initial equilibrium position starting at about 4.03 s, as shown in Fig. 3(c).

The linear vertical instability growth rate is calculated by fitting the experimental data with $z = z_0 + Ae^{\gamma(t-t_0)}$, where z is the plasma central position, z_0 is the origin plasma central position, γ is the instability growth rate, t is experimental time, and t_0 is the inital time when plasma starts to be displaced vertically. Only a small time window about 15 ms (about 2 times the instability growth time) is used as

the shadow area in Fig. 3 in fitting to assure the applicability of rigid displacement model with a small deformation of plasma configuration.

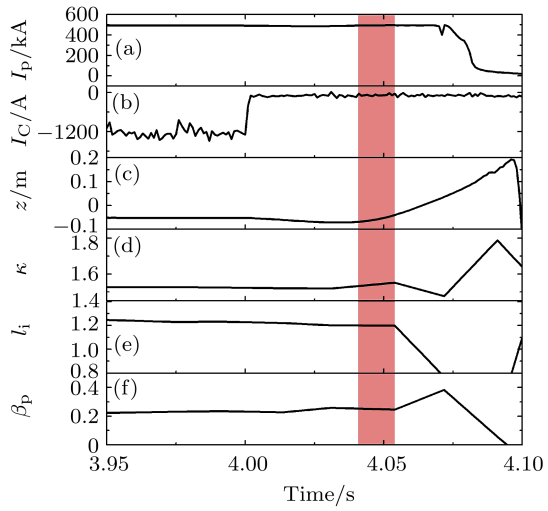


Fig. 3. (colour online) The time evolution of plasma current (a), active feedback current (b), plasma central position (c), elongation (d), internal inductance l_i (e), and poloidal plasma beta β_p (f) in shot 36795 on EAST.

3.2. Theoretical model

The rigid displacement model[3] is employed in the simulation. It is assumed in this model that the plasma current shifts rigidly with neither redistribution nor surface currents during the vertical displacement of the plasma column. Further assumptions are also made: negligible inertia, axisymmetric displacements, negligible horizontal-direction displacement, and constant total plasma current. In tokamak plasma experiments, these assumptions are valid in the case of small displacement.

The model can be described by the following circuit equation:[3,7,8]

$$L_{ss}I_s + R_{ss}I_s + \frac{\partial \psi_{sp}}{\partial z}z = V_s, \tag{1}$$

where L_{ss} is the mutual inductance matrix between mesh currents of the passive structure and PF coils, R_{ss} is the resistance matrix of the conductor structure, I_s and V_s are vectors of current and voltage of the conductor structure, respectively, ψ_{sp} is the flux at the conductor structure due to plasma current profile, $\dot{x}$ is the time derivative of x, and the subscript s and p refer to the passive structure and the plasma.

With negligible inertia, we obtain

$$L^*_{ss}I_s + R_{ss}I_s = V_s, \tag{2}$$

where

$$L^*_{ss} = L_{ss} - \frac{\partial \psi_{sp}}{\partial z}\frac{\partial z}{\partial I_s}$$

is the modified inductance matrix of the passive structure and PF coils including the effect of the plasma currents.

The growth rate of vertical instability can be written as

$$\gamma = \max\{\mathrm{eig}(-R^{-1}_{ss}L^*_{ss})\}, \tag{3}$$

where $-L^*R^{-1}$ is the state matrix of Eq. (2).

The stability margin (m_s) is defined as

$$m_s = \max\{\mathrm{eig}(-L^{-1}_{ss}L^*_{ss})\}. \tag{4}$$

The m_s is related to the passive structure and independent of resistance. Stability margin is approximately the ratio of the unstable growth time to the wall penetration time, $m_s \sim \tau_g/\tau_w$. The stability margin can be used for describing the distance from the ideal stability limit occurring at $m_s = 0$, which means that flux in the conductor structure is zero, conductor structure has no effect on plasma vertical displacement, and plasma column is displaced freely.[3,8] For effective vertical control, tokamak must operate above a minimum stability margin, and active feedback system response time must be less than instability growth time $\tau = 1/\gamma$.

3.3. Comparison between experiments and simulations

The passive plate resistance in case B is estimated in the range of 1 mΩ–3 mΩ. L^*_{ss} is calculated from the equilibrium configuration by EFIT.[11] The predicted instability growth rate is evaluated from Eq. (3).

The comparison between the observed growth rates and the predicted ones is shown in Fig. 4. The model predicted vertical instability growth rates accord well with the observed ones within the uncertainties in the resistance of the passive plate.

Compared with the results in case C without the passive plate, the vertical instability growth rates in case B are reduced by a factor of about 2, although the plasma parameters are similar in these two cases.

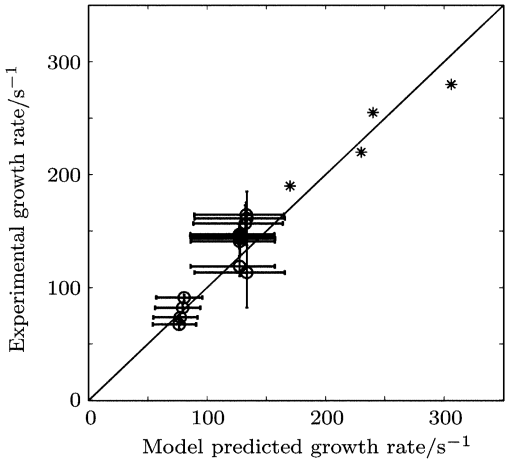


Fig. 4. Observed growth rate versus model predicted growth rate. The open circle represents the results with the passive plate resistance being 2 mΩ (case B), where the horizontal error bars denote uncertainties in resistance, and vertical error bars refer to experimental fitting errors. The star points represent the results without passive plates (case C) in Ref. [5].

4. Open loop numerical simulations

4.1. L/R time constants of the conduct structure

Figures 5 and 6 show the features of eddy currents in the conducting structure in EAST. The L/R time constants of the first 10 modes are presented in Fig. 5. The first up–down antisymmetric L/R mode has a dominant stabilization effect on vertical displacement control. Mode 1 is for case A, and mode 2 for cases B and C. The normalized current distributions of the first up–down antisymmetric L/R mode for cases A, B, and C are shown in Fig. 6. The time constant for vertical displacement control are 92.2 ms in case A, 13.1 ms in case B, and 12.2 ms in case C.

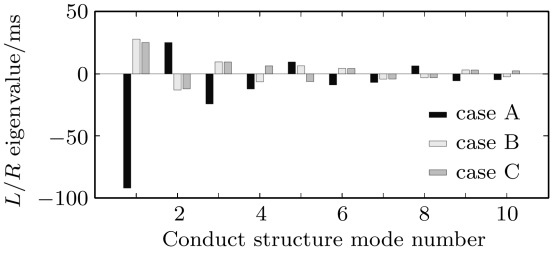


Fig. 5. Variation of the L/R time constant of each conduct structure eddy current mode (the first 10 modes, ordered by decreasing L/R time constant) with conducting structure mode number, where the positive and negative denote the up–down symmetric and up–down antisymmetric modes, respectively.

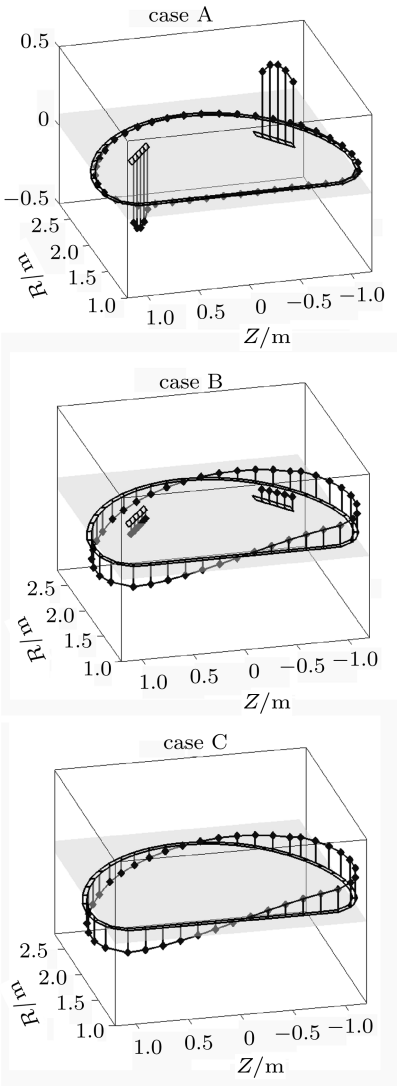


Fig. 6. Normalized current distribution of the first up–down anti-symmetric L/R eigenmode.

4.2. Predictions of stabilization benefits of passive plates on vertical instability

The used equilibrium configurations are generated from EFIT code based on EAST designed parameters. The plasma current and triangularity are fixed at $I_{\rm p} = 1$ MA, $\delta \approx 0.5$, and other effective parameters $\beta_{\rm p}$, κ, $l_{\rm i}$ are scanned. The stability margin and vertical growth rate are evaluated from Eqs. (3) and (4). The simulation results are presented in Figs. 7, 8, and 9.

It is seen in Figs. 7–9 that the vertical instability growth rates incline with κ and $l_{\rm i}$ increasing and $\beta_{\rm p}$ decreasing for all three cases.

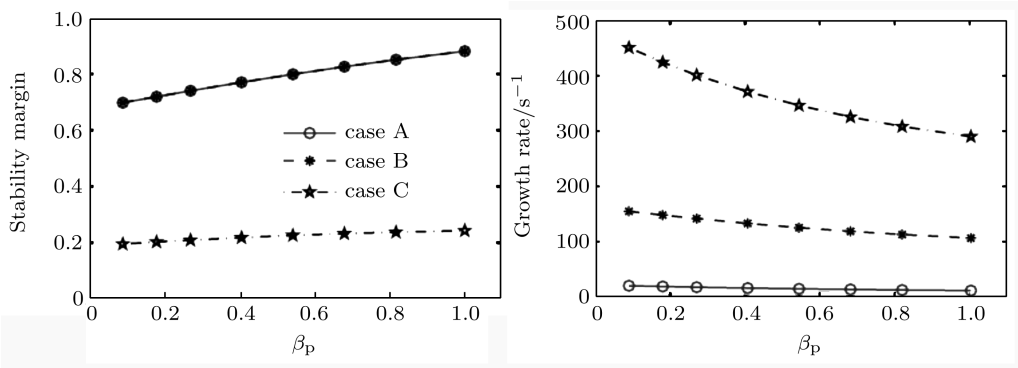


Fig. 7. Dependences of the stability margin (left) and vertical instability growth rate (right) on β_p with $\kappa = 1.93 \pm 0.02$, $l_i = 0.945 \pm 0.04$, $A = 3.95 \pm 0.02$.

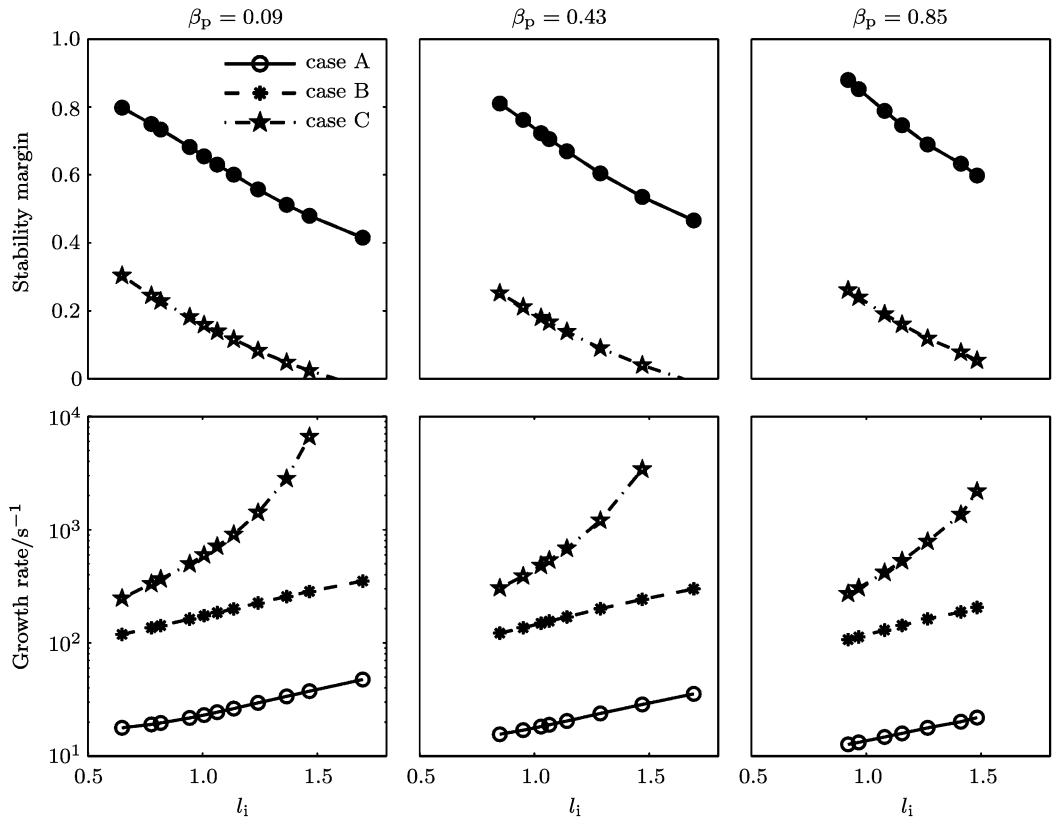
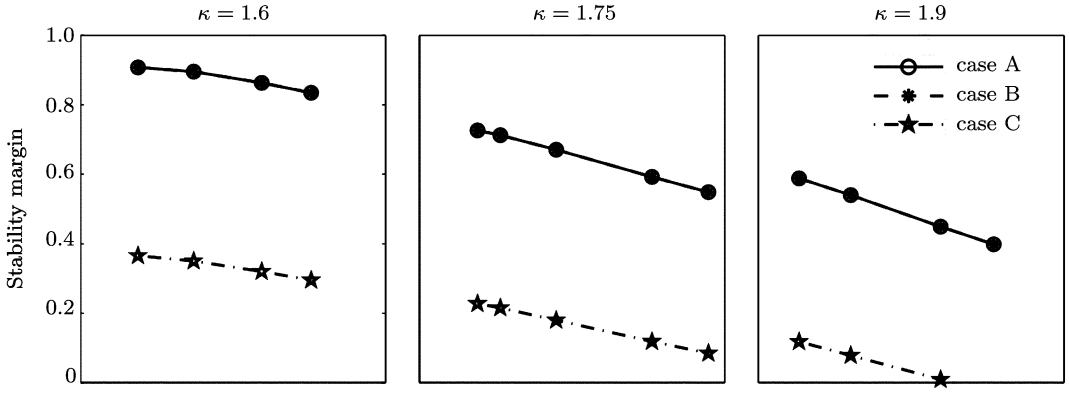


Fig. 8. Dependences of stability margin (top) and vertical instability growth rate (bottom) on l_i with $\kappa = 1.93 \pm 0.02$, $A = 3.95 \pm 0.02$, and $\beta_p = 0.09$ (left), $\beta_p = 0.43$ (middle), and $\beta_p = 0.85$ (right).



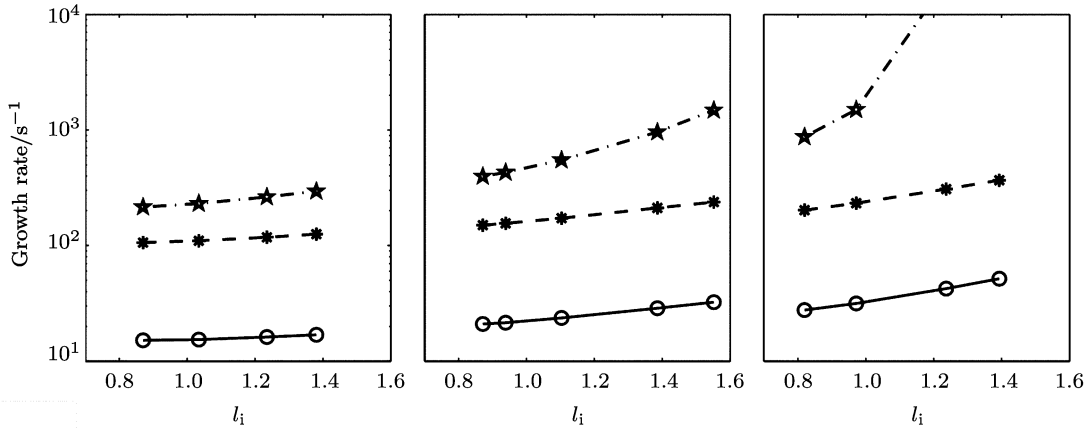


Fig. 9. Dependences of stability margin (top) and vertical instability growth rate (bottom) on l_i with $\beta_p = 0.43 \pm 0.02$, $A = 3.95 \pm 0.02$, and $\kappa = 1.6$ (left), $\kappa = 1.75$ (middle), and $\kappa = 1.9$ (right).

It is also clearly shown that the passive plate can benefit the stabilization of vertical displacements. The vertical instability growth rates are reduced by a factor of about 10 in case A and by a factor of about 2 in case B, compared with those in case C without passive plates.

Stability margin is the same in cases A and B due to its independence of the resistance of passive plates, and much larger than that in case C without passive plates. The stabilization effect of the passive plate becomes stronger for larger plasma parameters (κ, β_p, l_i), which implies that the operational window is enlarged by using passive plates.

5. Conclusion

The simulation results demonstrate that the stabilization is strengthened greatly in case A with the designed passive plates (as shown in Fig. 2), because its first up–down antisymmetric L/R time constant is much larger than that in case C without a passive plates (shown in Fig. 5), and the eddy currents in passive plates are closer to plasma. The much larger eddy current distribution (shown in Fig. 6) enhances the passive plate stabilization effect, which reduces vertical instability growth rates by a factor of about 10 compared with those in case A.

The passive plate in case B with the present design (as shown in Fig. 2) cannot change conduct structure eddy current decay time much (shown in Fig. 5), but eddy currents in passive plates (shown in Fig. 6) strengthen the coupling between plasma and the structure, which reduces vertical instability growth rates by a factor of about 2 compared with that in case B.

In summary, it is clearly seen from the comparison between experimental results and simulation ones that the passive plate in EAST can benefit the stabilization of vertical displacements, by increasing stability margin and reducing the vertical instability growth rate. Through passive plates and the same active feedback coils, the operational window is enlarged in tokamak. EAST has achieved 1-MA stable plasma discharges with present passive plates (case B).[12]

References

[1] Hender T C, Wesley J C, Bialek J, Bondeson A, Boozer A H, Buttery R J, Garofalo A, Goodman T P, Granetz R S, Gribov Y, Gruber O, Gryaznevich M, Giruzzi G, Günter S, Hayashi N, Helander P, Hegna C C, Howell D F, Humphreys D A, Huysmans G T A, Hyatt A W, Isayama A, Jardin S C, Kawano Y, Kellman A, Kessel C, Koslowski H R, Haye R J L, Lazzaro E, Liu Y Q, Lukash V, Manickam J, Medvedev S, Mertens V, Mirnov S V, Nakamura Y, Navratil G, Okabayashi M, Ozeki T, Paccagnella R, Pautasso G, Porcelli F, Pustovitov V D, Riccardo V, Sato M, Sauter O, Schaffer M J, Shimada M, Sonato P, Strait E J, Sugihara M, Takechi M, Turnbull A D, Westerhof E, Whyte D G, Yoshino R, Zohm H and the ITPA MHD, Disruption and Magnetic Control Topical Group 2007 *Nuclear Fusion* **47** 128

[2] Sharma A S, Limebeer D J N, Jaimoukha I M and Lister J B. 2005 *IEEE Transactions on Control Systems Technology* **13** 356

[3] Portone A 2005 *Nuclear Fusion* **45** 926

[4] Wan B 2009 *Nuclear Fusion* **49** 104011

[5] Qian J P, Wan B N, Shen B, Walker M L, Humphreys D A and Xiao B J 2009 *Chin. Phys.* B **18** 2432

[6] Qian J P, Wan B N, Shen B, Lao L L, Xiao B J, Li J G, Lin S Y and Luo Z P 2009 *Chin. Phys.* B **18** 1172

[7] Albanese R, Coccorese E and Rubinacci G 1989 *Nuclear Fusion* **29** 1013

[8] Humphreys D, Casper T, Eidietis N, Ferrara M, Gates D, Hutchinson I, Jackson G, Kolemen E, Leuer J and Lister J 2009 *Nuclear Fusion* **49** 115003

[9] Qian J P, Wan B N, Shen B, Xiao B J, Sun Y W, Shi Y J, Lin S Y, Li J G and Gong X Z 2008 *Plasma Sci. & Technol.* **10** 290

[10] Ji X 2012 *Plasma Sci. & Technol.* (in press)

[11] Lao L, St John H, Stambaugh R, Kellman A and Pfeiffer W 1985 *Nuclear Fusion* **25** 1611

[12] Qian J P, Gong X Z, Li J A, Wan B N, Ling B L, Shen B A, Ti A, Zhong G Q, Lin S Y, Chang J F and Wang H Z 2011*Plasma Sci. & Technol.* **13** 1